nature structural & molecular biology

Conformational dynamics of the KcsA potassium channel governs gating properties

Kent A Baker[1,3], Christos Tzitzilonis[1,3], Witek Kwiatkowski[1], Senyon Choe[1] & Roland Riek[1,2]

K^+ channels conduct and regulate K^+ flux across the cell membrane. Several crystal structures and biophysical studies of tetrameric ion channels have revealed many of the structural details of ion selectivity and gating. A narrow pore lined with four arrays of carbonyl groups is responsible for ion selectivity, whereas a conformational change of the four inner transmembrane helices (TM2) is involved in gating. We used NMR to examine full-length KcsA, a prototypical K^+ channel, in its open, closed and intermediate states. These studies reveal that at least two conformational states exist both in the selectivity filter and near the C-terminal ends of the TM2 helices. In the ion-conducting open state, we observed rapid structural exchange between two conformations of the filter, presumably of low and high K^+ affinity, respectively. Such measurements of millisecond-timescale dynamics reveal the basis for simultaneous ion selection and gating.

The simplest structural definition of ion channel gating is the ability to alternate, in a signal-dependent way, between states that selectively permit the flow of ions (open) or do not (closed). In the closed state, generally a default state, K^+ channels inhibit ion flow with high efficacy. In the open state, two opposing tasks must be carried out near the diffusion limit: ion selection and permeation[1]. Energetically, ion selection requires spatial coordination that favors K^+ over other cations, whereas permeation requires the rapid release of the cation from these recognition sites. This 'hold-and-release' feature underlies the unique structural and dynamical properties of the channel.

Crystal structures of K^+ channels of prokaryotic origin (KcsA[2], MthK[3], KirBac1.1 (ref. 4), KvAP[5] and NaK[6]) have revealed a universal structural framework for these tasks. To explain ion selectivity, the structures show a narrow filter composed of four successive layers of main chain carbonyl oxygen atoms, which act as surrogate waters for the dehydrated K^+ ions (1.35-Å radius) as they pass through the filter. This unique spatial geometry results from the signature filter amino acid sequence, Gly-Tyr-Gly, in which the two glycines enable positive ϕ/ψ angles of the protein backbone so that the K^+-coordinating carbonyl oxygens can all point inward to the pore axis simultaneously[7] to perform ion selection[8,9]. For gating of the channel, the pore-lining C-terminal ends of the inner transmembrane helix 2 (TM2) helices converging near the cytoplasmic junction have been proposed to occlude the ionic flow[10–13]. However, mutagenesis studies[14–16] and molecular dynamic simulations[9,17] have suggested that the filter also has an important structural and dynamical role in gating. In the present study, we have used multidimensional NMR spectroscopy with the prototypical K^+ channel KcsA from *Streptomyces lividans* to elucidate the conformational and dynamic changes related to gating and conduction on timescales relevant to these channel activities.

RESULTS

Secondary structure of KcsA in open and closed states

To compare the structures of KcsA's open and closed states, we made use of the pH dependency of these states. KcsA is closed at pH 7 but open at pH 4, at which it largely inactivates after several seconds[14] but remains open 15% of the time. We examined a KcsA variant carrying a triple mutation that enables toxin binding (Q58A T61S R64D)[18], termed KcsA(tox). We made all measurements of tetrameric KcsA in a foscholine detergent micelle, which allows for the pH to be titrated between pH 7 and pH 4. The foscholine–KcsA complex closely mirrors a membrane-embedded functional channel, as it binds agitoxin II (**Supplementary Fig. 1** online), forms a tetramer that can be observed by SDS-PAGE and analytical ultracentrifugation (data not shown), and has a rotational correlation time, τ_c, of 60 ns, consistent with the expected molecular weight of ~130 kDa for the KcsA–detergent complex (**Supplementary Fig. 2a**,**b** online). This correlation time is in agreement with a relaxation study of a truncated version of KcsA measured at 50 °C (ref. 19).

Using a combination of TROSY-based triple-resonance experiments[20], TROSY-based NOESY experiments and selective isotope labeling (**Supplementary Fig. 3** online), we have obtained ~85% of the sequential backbone assignments of full-length KcsA(tox) at pH 7 (**Fig. 1**). A residue-specific secondary structure analysis based on positive $^{13}C\alpha$ chemical shift deviations from a random coil (**Fig. 1a**), amide-H_2O exchange (**Supplementary Fig. 4b** online) and protein-detergent NOEs (**Supplementary Fig. 4a**) revealed the presence of the following helices: transmembrane helix 1 (TM1), comprising residues 30–51 (residues 24–51 in the crystal structure); the P-helix, comprising residues 64–74 (62–73 in the crystal structure); and the inner TM2, comprising residues 87–118 (86–121 in the crystal

[1]Structural Biology Laboratory, The Salk Institute, La Jolla, California 92037, USA. [2]Laboratory of Physical Chemistry, Swiss Institute of Technology (ETH) Zurich, CH-8093 Switzerland. [3]These authors contributed equally to this work. Correspondence should be addressed to S.C. (choe@salk.edu) or R.R. (riek@salk.edu).

Received 11 May; accepted 10 September; published online 7 October 2007; doi:10.1038/nsmb1311

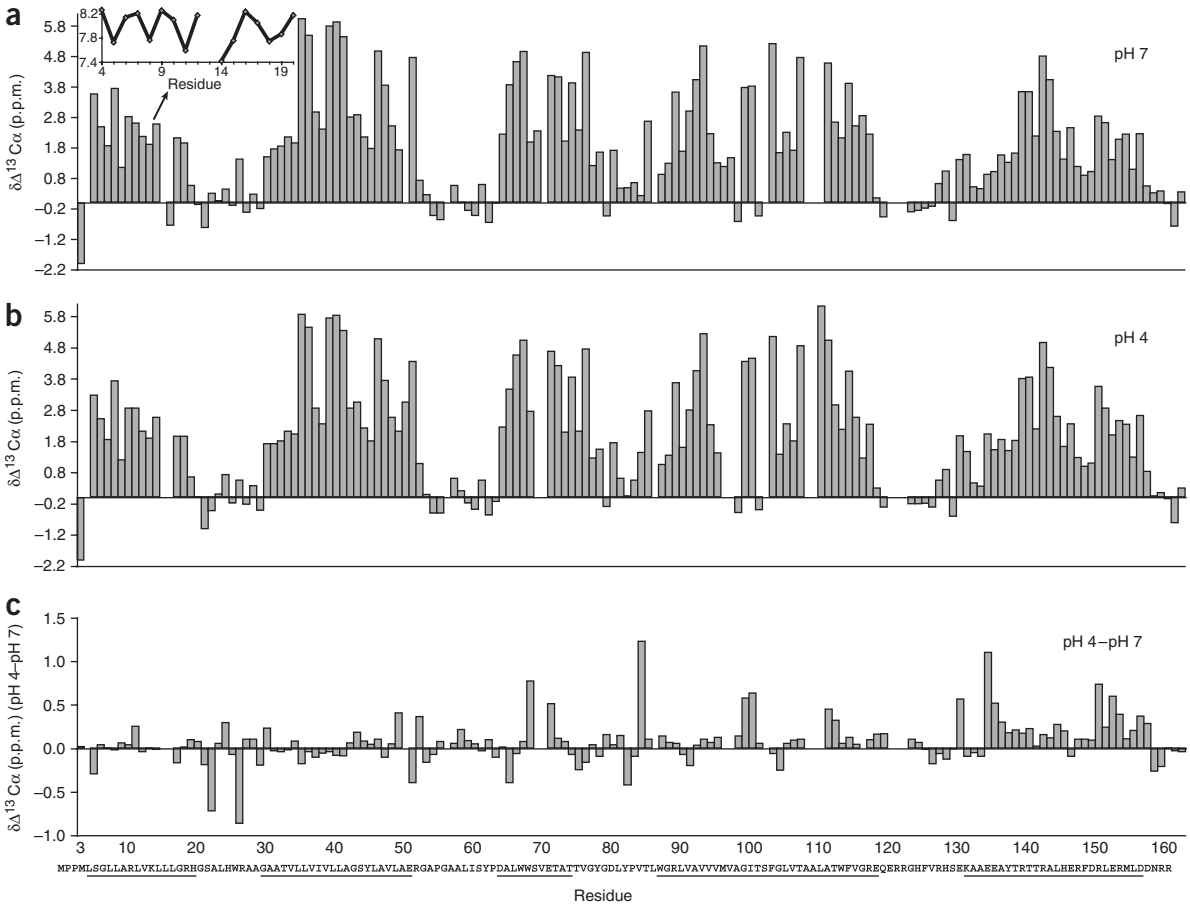

Figure 1 Secondary structure of KcsA(tox) in the closed and open conformations. (**a**,**b**) Deviations of the $^{13}C\alpha$ chemical shifts from corresponding random-coil chemical shifts at pH 7 (closed conformation; **a**) and pH 4 (open conformation; **b**). Values larger than 1.5 p.p.m. are indicative of α-helical secondary structure, denoted by underline below panel **c**. Inset in **a** shows the ^{1}HN chemical shifts of the N-terminal helix. The wave pattern is indicative of an amphipathic helix. (**c**) Difference of the $^{13}C\alpha$ chemical shifts between the open and closed conformations. On the basis of these data, we identified structural changes between the closed and open conformations at the C terminus of TM2 and in the cytoplasmic C-terminal helix. Below, primary sequence of KcsA with α-helices underlined.

structure)[2] (see also **Supplementary Table 1** online). Both transmembrane helices are embedded in foscholine micelles, as evidenced by detergent-protein NOEs and the lack of water-protein exchange peaks (**Supplementary Fig. 4** and **Supplementary Table 2** online). Only the amide of Thr33 of TM1 is in fast exchange with water, which is consistent with the presence of an ordered water molecule in the high-resolution crystal structure[21].

A previously proposed N-terminal, membrane-attached amphipathic helix comprising residues 5–20 is evident in our results[22]. In particular, the wave pattern of the amide proton chemical shifts (**Fig. 1a**) and the mixed behavior of detergent-protein NOEs and water exchange peaks (**Supplementary Fig. 4**) suggest that this helix is partially embedded in the membrane. A cytoplasmic C-terminal helix comprising residues 131–156 (refs. 19,22), previously delineated by EPR and NMR spectroscopy, is also apparent. The length of the C-terminal helix of full-length KcsA is thus considerably longer in the present NMR structure than in a previous one by another group[19] (**Supplementary Table 1**). We attribute this difference to the high temperature (50 °C) and harsh detergent used in the earlier study[19], which may partially unfold the cytoplasmic helix. The N- and C-terminal helices are either truncated or disordered in all available crystal structures. The C-terminal helix is solvent exposed, as evidenced by the high degree of exchange between corresponding amides and H_2O and the absence of detergent-protein interactions (only two aromatic residues show detergent-protein NOEs, probably owing to nonspecific hydrophobic interactions in the highly concentrated samples and/or the presence of about 1.5 mM free foscholine). Overall, the secondary structure of full-length KcsA derived from the NMR data is in excellent agreement with existing models and crystal structures[2,21,22].

Next, we repeated the NMR studies at pH 4. Again, we obtained ~85% of the sequential backbone assignments of full-length KcsA(tox). Comparison of the $^{13}C\alpha$ chemical shift deviation from a random coil for the channel at pH 4 with that at pH 7 (**Fig. 1**) reveals few secondary structural differences between the two pH conditions. The difference plot shows that the C-terminal helix is more prominent at pH 4 than at pH 7. This finding is supported by the slower amide-H_2O exchange observed in the C-terminal helix at pH 4 when compared to pH 7 (**Supplementary Fig. 4b**,**d**; however, this data must be interpreted with caution, as the intrinsic exchange rates of amides at pH 4 are three orders of magnitudes slower than at pH 7). The chemical shift difference plot further suggests subtle structural changes between the conformations at pH 7 and at pH 4 in the C-terminal half of TM2 between residues 96 and 116 (**Fig. 1c**).

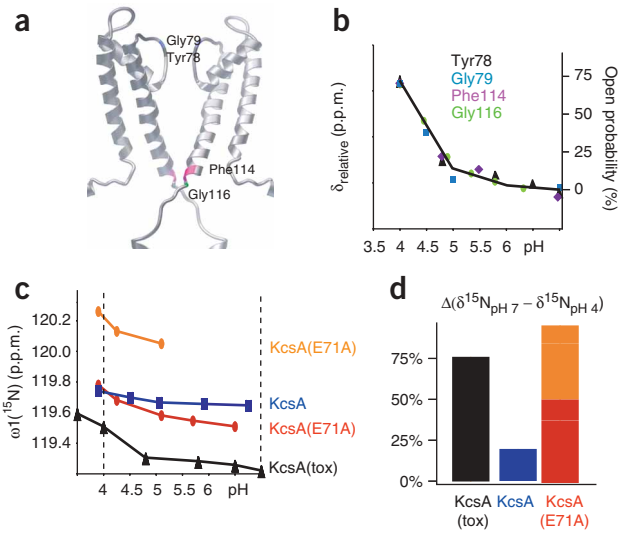

Figure 2 Correlation between functional and structural data for KcsA. (**a**) Residues Tyr78 (black), Gly79 (blue), Phe114 (purple) and Gly116 (green), for which pH-dependent chemical shifts correlated with functional data, are highlighted on the three-dimensional model of KcsA. (**b**) Relative chemical shift changes (left *y*-axis) of Tyr78 (black triangles), Gly79 (blue squares), Phe114 (purple diamonds) and Gly116 (green circles) of KcsA(tox) are plotted against pH. Superimposed is the open probability of KcsA (right *y*-axis) plotted against pH (black line), as measured in another study[23]. The absolute pH-dependent ^{15}N chemical shift changes of the residues are given in **Supplementary Table 3**. (**c**) Chemical shift change versus pH for Tyr78 of wild-type KcsA and indicated variants. (**d**) Relative open probabilities of KcsA, KcsA(tox) and KcsA(E71A), calculated from the relative chemical shift differences of Tyr78 between pH 7 and pH 4 assuming a model with two states between the open (pH 4) and closed (pH 7) conformations. The relative chemical shift differences are shown as percentages of the value for the open conformation.

Structural differences between the open and closed states

To detect detailed structural and dynamical differences between the open and closed states of KcsA, we performed pH titration studies on residue-specific ^{15}N-^{1}H moieties from pH 7 to pH 4 (and lower) (**Fig. 2** and **Supplementary Fig. 5** online). Many pH-dependent chemical shift changes were evident (**Supplementary Table 3** and **Supplementary Fig. 5**). We then compared the titration curves with pH-dependent functional data from a previous study in which the probability of channel opening was measured in liposomes[23] and showed a very characteristic curve (**Fig. 2b**, black line). Demonstrating a correlation between the NMR data and the functional titration data is important in validating conclusions from the NMR experiments, as local protonation events may result in chemical shift changes of no functional importance. Furthermore, correlation is a good indication that changes in residue-specific NMR signals of isolated KcsA tetramers in detergent micelles accurately reflect the pH-dependent gating behavior of KcsA in the cell membrane.

Supplementary Figure 5 and **Fig. 2a,b** show data from a selection of the more than 100 titration curves we analyzed. These results demonstrate the presence of a large variety of pH-dependent chemical shift changes. We find that the pH-dependent chemical shift changes of Phe114 and Gly116 at the C-terminal end of TM2, and of Tyr78 and Gly79 in the selectivity filter, indeed correlate very well with the functional profile (**Fig. 2b**). The data support our hypothesis and suggest that conformational changes occurring both at the C terminus of TM2 and the filter are part of the mechanism of gating (**Fig. 2a**). This is in agreement with the secondary structure analysis above (**Fig. 1**) and earlier studies showing that local conformational changes in TM2 (refs. 11,13,14) and in the filter[10,16,24] accompany the transition from the open to the closed state.

To further examine the pH-induced conformational changes of the filter between the open and closed states, we measured ^{3}J(Hα,HN) scalar coupling to directly determine the backbone ϕ-angles in the filter through the Karplus relationship[25] (**Fig. 3**). Despite a low signal-to-noise ratio, the ^{3}J(Hα,HN) scalar coupling of Tyr78 could be reliably determined. The ^{3}J(Hα,HN) of Tyr45 was also measured, as a positive control. Tyr45, located in TM1, has $\phi \approx -65^{\circ}$ in the crystal structures[21], which corresponds well, through the Karplus relationship, to the measured ^{3}J(Hα,HN) of 5 ± 1 Hz (**Fig. 3**). For Tyr78 in the closed conformation at pH 7 in the absence of K^+, ^{3}J(Hα,HN) is 8 ± 1 Hz, indicating either $\phi < -90^{\circ}$ or the presence of conformational heterogeneity. Upon addition of 10 mM K^+, the ^{3}J(Hα,HN) of Tyr78 dropped to below 3 Hz, corresponding to $\phi > -50^{\circ}$. This ϕ-angle of Tyr78 deduced from the ^{3}J(Hα,HN) value is in good agreement with the corresponding value from the crystal structures of KcsA[21] (**Fig. 3**). We considered the most important measurement of the ^{3}J(Hα,HN) scalar coupling series to be the determination of the ϕ-angle of Tyr78 in the low-pH, open state of KcsA, as no high-resolution data

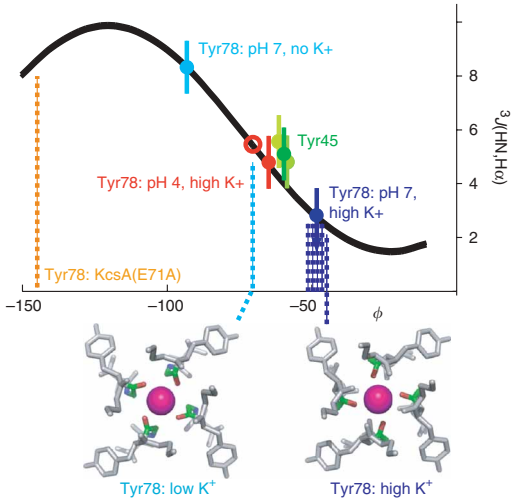

Figure 3 Conformational difference in the backbone angle ϕ of Tyr78 between the conducting (pH 4) and nonconducting (pH 7) conformations of KcsA(tox). (**a**) The backbone angle ϕ of Tyr78 at pH 4 in the presence of K^+ and at pH 7 in the presence or absence of K^+, as calculated from $^{3}J(^{1}HN,^{1}H\alpha)$ scalar coupling measurements using the Karplus relationship (represented by curve). Dotted lines mark the ϕ-angles of Tyr78 in the crystal structures of KcsA in the presence of low K^+ (cyan)[21] and high K^+ (blue)[21], and in the crystal structure of KcsA(E71A) in the alternative open conformation (orange)[14]. The relationship between $^{3}J(^{1}HN,^{1}H\alpha)$ scalar coupling and the ϕ-angle of Tyr45 is shown for comparison; in all the crystal structures, Tyr45 is in a helical conformation with $\phi \approx -60^{\circ}$. Red circle indicates a scaled scalar coupling at pH 4, which takes into account that Tyr78 of KcsA(tox) is in the low-affinity state with a probability of only 75% (see **Fig. 2**). The experiments were repeated at least three times. Error bars show s.d. Below, three-dimensional representations of the variations in Tyr78 angles at pH 7 and pH 4, from crystal structures at low and high K^+ concentrations[21]. K^+ is shown as a pink sphere coordinated by the filter oxygens of Gly77 (red). Tyr78 backbone is in green.

Table 1 Correlation between functional and dynamical data for KcsA variants at pH 4

	KcsA	R64, no K^+	R64	E71A
Macroscopic functional data[a]				
Open probability (%)	10–15	ND	70	100
Mean open time (ms and Hz)	30 ms (33 Hz)	ND	120 ms (8 Hz)	100 ms (10 Hz)
Local NMR data[b]				
Tyr78	20%	75%, 500 ± 50 Hz	75%, 100 ± 10 Hz	75% (0.6) and 100% (0.4)[c], 10 ± 5 Hz
Gly79	ND	95%	95%, 40 ± 10 Hz	ND
Phe114	ND	90%, 2–4 kHz	ND	ND
Gly116	90%, >2 kHz	90%, 3–4 kHz	90%, 3–4 kHz	ND

ND, not determined.
[a]Functional data from refs. 14 and 23. [b]We analyzed pH titration data assuming a two-state model with a local nonpermeable state at pH 7 and a local permeable state at low pH. The occupancy of the local nonpermeable state at pH 4 is given in %. The exchange rates between the local permeable and nonpermeable states were determined by line-broadening analysis and are listed in Hz. The accuracies of the rates were estimated on the basis of repetitive measurements and analysis. [c]The E71A mutant has two distinct conformations at pH 4, in a ratio of 0.6 to 0.4. Hence, two values are given.

are available for this state. In the presence of 10 mM K^+ at pH 4, a ^3J(Hα,HN) scalar coupling of 5 ± 1 Hz was measured, which corresponds to $\phi \approx -70^\circ$. Our extraction of the ϕ-angle from ^3J(Hα,HN) at this pH takes into account that Tyr78 in KcsA(tox) is open only about 75%, as determined from chemical exchange analysis (see below). Hence, the structural change in the filter from the closed to the open state includes a change in the mean ϕ-angle of Tyr78 of about 20° (from –70° to –50°). Although thermal fluctuations of the atoms by 1 kT can change the angle by a similar amount, our measurement fundamentally shows a stereochemical shift driven by pH in the presence of K^+. This subtle but clear change in angle between the permeating and nonpermeating conformations of the filter provides a physical basis to explain possible changes in the K^+-binding affinity of the filter, which most probably shifts from a high-affinity conformation in the closed state to a lower-affinity conformation in the open state. Although no angles could be determined for Gly79 because of the sensitivity limits of the NMR experiment, the pH-dependent chemical shift changes of Gly79 (**Fig. 2b**) are also consistent with a conformational change away from the ion-bound conformation of Tyr78 at pH 7.

Conformational dynamics of KcsA in the open state

To explore the dynamics involved in channel conductance, we studied the conformational exchange dynamics of KcsA, also examined by others[19,26,27], using NMR spectroscopy. Our variants are all closed at pH 7, but they differ in open probability and mean open time at pH 4 (**Table 1**). At pH 4, wild-type KcsA has an open probability of only ~15%, with a mean open time of 30 ms; the mutant R64A has an open probability of 70%, with a mean open time of 120 ms; and E71A is almost always open, with a mean open time of 100 ms (ref. 14). **Figure 2c** and **Figure 4** show titration measurements of Tyr78 from wild-type KcsA, KcsA(E71A), and KcsA(tox) with the R64D mutation mimicking the R64A variant. Analysis of these NMR titration studies between pH 7 and pH 4 using a two-state model reveals that at pH 4, Tyr78 of wild-type KcsA or KcsA(tox) is in its nonpermeating configuration 20% or 75% of the time and in its permeating configuration 80% or 25% of the time, respectively. The situation for Tyr78 in KcsA(E71A) at pH 4 is more complex, as Tyr78 shows two distinct cross-peaks in the NMR spectra below pH 5.5, with a ratio of 2:1 at pH 4, indicative of a very slow exchange between two conformations (**Fig. 4**). The presence of two distinct conformations of Tyr78 in KcsA(E71A) is consistent with the crystal structures of KcsA(E71A)[14]. The NMR and crystallography data together suggest that the major conformation is in the local permeating state with an open probability of 80% and the minor conformation is in a different permeating state all the time (**Fig. 2c** and **Fig. 4**). Therefore, the good correlation between the macroscopic open probabilities of these KcsA variants and the corresponding probabilities derived from chemical shift changes of Tyr78 further supports the idea that the role of the selectivity filter includes gating by alternating configurations (**Table 1**). The importance of the selectivity filter in gating is further supported by the observation that the local open probability of Gly116 at the C terminus of TM2 does not differ between KcsA and KcsA(tox) (**Table 1**).

Line-broadening analysis of the titration curves of KcsA(tox) reveals further details of the local stereochemical exchange rates between the alternating conformations, which are both present in the ion-conducting conformational state of the channel at pH 4. At pH 4, the ^{15}N-^{1}H moiety of Tyr78 exchanges in the absence of K^+ at a rate of ~500 Hz between permeating and nonpermeating conformations. In the presence of K^+, the exchange rate of Tyr78 slows to ~100 Hz. This rate difference not only allows us to estimate that K^+ binding to Tyr78 is energetically favored by a $\Delta\Delta G$ of 1–2 kcal mol^{-1}, but also supports the idea that the permeating and nonpermeating conformations are the low- and high-affinity states, respectively. Further dynamical analysis reveals that at pH 4, Gly79 also exchanges between two putative configurations, one high and one low affinity, with a 50-Hz exchange rate and 90% occupancy in the low-affinity configuration. The conformational exchange at the C terminus of TM2 between the pH 7 and pH 4 states is on the order of 2–4 kHz with an open probability of 90%, as determined for Phe114 and Gly116 (**Table 1**). The difference in occupancies as well as in exchange rates demonstrates that the observed dynamics in the filter, particularly at positions 78 and 79, and the changes at the C terminus of TM2 are partly independent of each other.

DISCUSSION

pH triggers for KcsA conductance

The pH-dependent conductance of KcsA indicates that a conformational trigger to open the channel occurs in a low-pH environment. The NMR studies suggest that changes in the C terminus of TM2 might be such a pH trigger. This proposal is based on the observation that the C terminus of TM2, as well as the filter residues Tyr78 and Gly79, are pH sensitive between pH 7 and 6, with similar pH dependence (**Fig. 2b**). In this pH range, only the side chains of histidine and, in rare cases, glutamate and aspartate are titratable. However, the glutamate and aspartate residues of KcsA seem to have pKs between 3 and 5, as suggested by molecular dynamics simulations[28,29] and by the pH-dependent chemical shift changes we observed at aspartate and glutamate, and/or their neighboring residues (**Supplementary Table 3**). Hence, the only titratable groups in this pH range seem to be the side chains of histidines, which are absent in the transmembrane and extracellular segments of TM2 but present at its

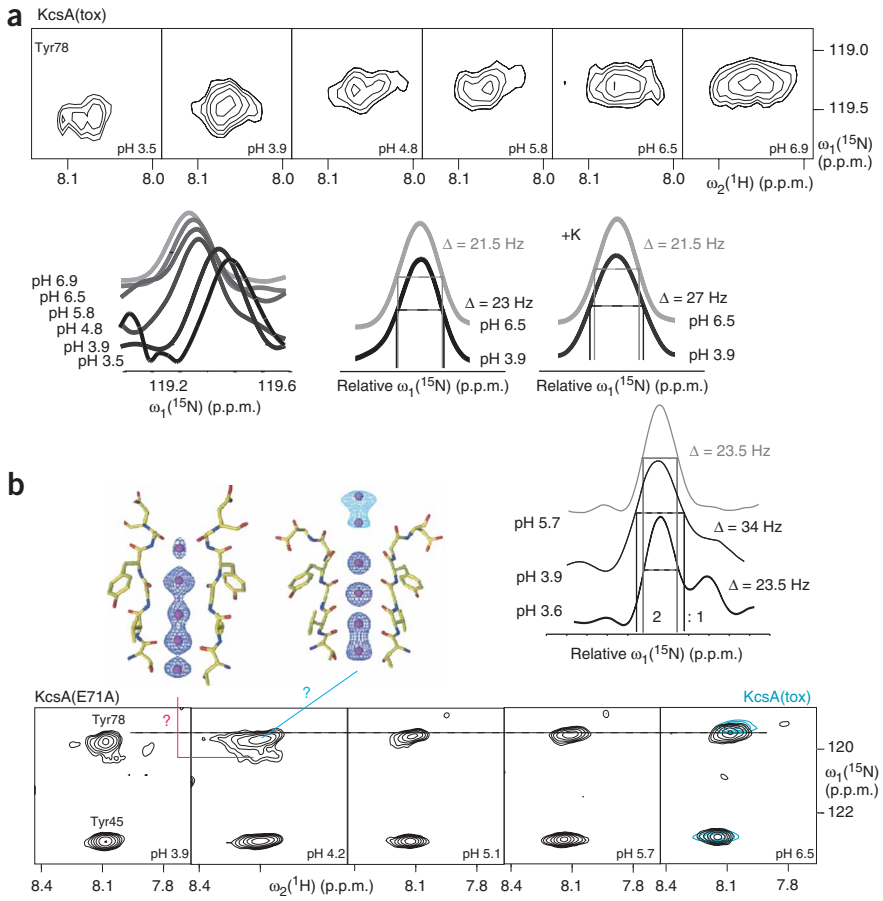

Figure 4 pH titration of ^{15}N-Tyr–labeled KcsA(tox) in the presence of K^+, and KcsA(E71A) in the absence of K^+. (**a**,**b**) The cross-peaks of Tyr78 of KcsA(tox) (**a**) and KcsA(E71A) (**b**) in the ^{15}N-^{1}H TROSY spectra are shown at different pHs, both as two-dimensional representations and in cross-sections. In cross-sections, the line-broadening effect of conformational exchange is indicated. In **b**, the two filter conformations from the crystal structures of KcsA(E71A) are shown[14]. Question marks connecting these conformations with the NMR peak doubling denote that there is no direct information available as to whether the peak doubling originates from the same structural plurality observed in the crystals.

C terminus. This indicates a probable conformational link between the C terminus of TM2 and the filter. The conformational propagation between the two could be important in coordinating gating actions for conductance.

The present NMR studies also suggest that the complex hydrogen bond network between Tyr78, Gly79, Glu71 and Asp80 is another pH-sensitive trigger for conductance. As shown by a comparison of the exchange rates between the permeating and nonpermeating conformations of Tyr78 in wild-type KcsA (500 Hz) and KcsA(E71A) (10 Hz) (**Table 1**), the mutation E71A costs ~4 kcal mol^{-1} of energy for K^+ binding at Tyr78. The energy cost is equivalent to the loss of the hydrogen bond between Glu71 and Tyr78 and the water-mediated hydrogen bond between Glu71 and Asp80 in KcsA(E71A)[14], supporting the idea that the hydrogen bond network between Tyr78, Glu71, Asp80 and Gly79 is also involved in gating. As Glu71 and Asp80 are two residues that can be titrated in the pH range between 5 and 4, their protonation should influence the gating behavior, and they could contribute as additional pH-sensitive triggers for regulation of channel conductance by a long-range network of interactions[12,15].

KcsA channel conductance

The solution-state NMR studies presented here, in combination with crystal structures and other biophysical studies[2,15,21,30], consistently indicate that in the nonconducting conformation of KcsA at pH 7, K^+ is bound tightly by the coordinating oxygens of the selectivity filter, and that the C-terminal parts of the four TM2 helices converge near the cytoplasmic junction, acting as a barrier to further prevent ionic flow. In the conducting state at pH 4, in contrast, KcsA undergoes millisecond-timescale conformational exchange between locally permeating and nonpermeating conformations of the filter and between two conformations at the C-terminal end of TM2. The dynamics of this exchange between alternative stereochemical configurations in the filter provides a physical basis for simultaneous K^+ conductance and gating. A stochastic model of the selectivity filter can be conceived in which the channel alternates between a cation-bound conformation (to hold ions) and a cation-free, conducting conformation (to release ions).

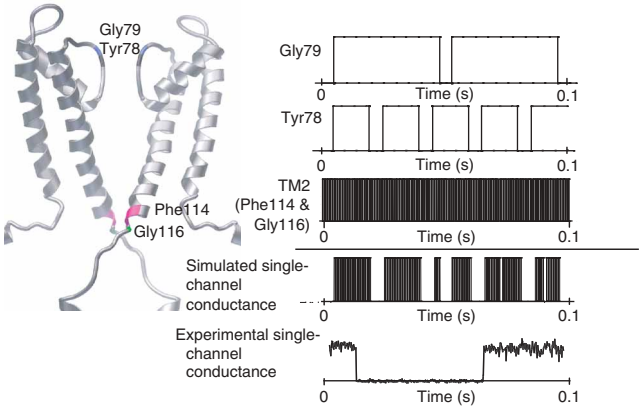

Figure 5 Channel conductance modeled on the basis of different exchange rates of the filter residues and the C terminus of TM2. The conformational exchange rates of Gly79, Tyr78 and the C terminus of TM2 are translated into a step function comprising two states, 0 for a locally nonpermeable state and 1 for a locally permeable state. Under the assumption that local conformational exchanges are independent of one another, the channel conductance can be modeled by multiplying the three step functions shown below. It is likely that there are additional conformational exchanges between locally nonpermeable and permeable states at the filter residues Thr-Thr-Val, which would substantially further influence the final channel conductance profile. The modeled channel conductance is compared with the experimentally measured single-channel conductance of KcsA(R64A) in symmetric KCl (200 mM KCl, pH 4.0, +150 mV). This experimental data was kindly provided by E. Perozo (University of Chicago) and is similar to the channel conductance measured in another study[14].

This model is conceptually consistent with a previously proposed mechanism for ion selection and gating of the filter[31], in which the channel alternates between an ion-selective, cation-bound, nonconducting conformation and a cation-free, conducting conformation. This model is sufficient to explain both ion selection and gating[13] and is now supported by direct experimental evidence. On an independent timescale, at pH 4, the C-terminal part of TM2 undergoes a conformational exchange between the closed and open states with a rate of ~3 kHz, most probably accompanied by a conformational change of the cytoplasmic helices, which are packed tighter at low pH. By simply combining the rates of exchange at the filter and at the TM2 randomly, we were able to simulate intra- and interburst gating profiles that match qualitatively what has been experimentally measured for typical ion-selective channels[14] (**Fig. 5**). In contrast to the slow-acting gating of the filter, the gating of TM2 is largely responsible for the fast-acting intraburst property of conductance. (Note that this simulation oversimplifies channel conductance, as it assumes completely uncorrelated conformational exchange dynamics, lacks the influence of the other filter residues Thr-Thr-Val on conductance, and was measured in the absence of voltage.)

Taking these results together, we propose that ion selection and permeation are two interlocked features of the selectivity filter that are physically governed by local exchange dynamics between its high- and low-affinity configurations, in addition to the conformational dynamics of TM2. These two respective configurations of the filter are most probably the K^+-holding and K^+-releasing states during ion conduction, the switch between which is stochastic by nature.

METHODS

Protein production. Protein was produced using a pET-28a vector containing the coding sequence of full-length KcsA fused to a thrombin-cleavable N-terminal hexahistidine tag. We introduced mutations of this sequence using QuikChange mutagenesis (Stratagene). Protein was expressed in cells of the *Escherichia coli* strain BL21(DE3) for uniform labeling or DL39(DE3)[32] for amino acid–specific labeling. We increased the yield by growing the cell mass in rich unlabeled media then transferring it into a smaller volume of labeling media just before induction, as described[33].

After protein expression, we lysed cells with sonication and pelleted membranes by centrifugation. We extracted KcsA from the membrane using 40 mM Mega-9 detergent along with gentle sonication. We then cleared this extraction mixture by centrifugation and applied it to a nickel–nitrilotriacetic acid column. Detergent was exchanged to 5 mM *n*-dodecylphosphocholine (foscholine) while the protein was bound to the resin. After detergent exchange, we eluted the protein by lowering the pH to 4.0. Fractions containing the protein were immediately adjusted to the desired pH before concentration. Before data collection, we concentrated and exchanged the protein by ultrafiltration into a final buffer of 20 mM Bis-Tris (pH 7.0) or 10 mM sodium acetate (pH 4.0), along with 5 mM foscholine. Maintaining an optimal ratio of protein to detergent was essential to produce good-quality spectra.

Nuclear magnetic resonance spectroscopy. We recorded spectra of ^{1}H-^{15}N TROSY, ^{15}N-^{1}H TROSY-HNCA[34], an optimized TROSY-based HN(CO)CA, and ^{15}N-resolved TROSY ^{1}H-^{1}H NOESY (mixing time 200 ms) with 70% ^{2}H,^{13}C,^{15}N-labeled KcsA(tox) on a Bruker Avance 700 spectrometer equipped with a cryoprobe at 37 °C for samples at both pH 4 and pH 7. ^{1}H-^{15}N TROSY spectra of amino acid–specific, ^{15}N-labeled (on either tyrosine, phenylalanine, leucine, valine or aspartate individually), ^{2}H-labeled KcsA(tox) channels were measured to identify amino acid residues unambiguously. In addition, we collected ^{1}H-^{15}N TROSY data for ^{15}N-Tyr, ^{2}H-labeled KcsA(tox) with an additional Y78F mutation (KcsA(tox,Y78F)), to identify Tyr78's cross-peak (**Supplementary Fig. 3**). For the pH and K^+ titration measurements, we collected ^{1}H-^{15}N TROSY data after the addition of sodium acetate or KSO_4. Relaxation of ^{19}F-Tyr KcsA(tox) was measured on a 500-MHz Bruker Avance spectrometer with a ^{1}H,^{19}F dual probe at pH 7 in presence of 10 mM K^+. We acquired 1D T1, T1ρ(CPMG) measurements at 14,000 Hz were acquired. A 1D ^{19}F spectrum of ^{19}F-Tyr KcsA(tox,Y78F) was measured to identify the ^{19}F resonance of Tyr78. T1 and T1ρ of ^{19}F-Tyr78 (**Supplementary Fig. 2**) are 0.6 s and 11 ms, respectively, yielding a rotational correlation time of ~60 ns, which accords well with the expected molecular weight of ~130 kDa for the detergent–protein complex. The isolated tetrameric KcsA at a subunit concentration of 0.7 mM remains fully soluble in the presence of 5 mM foscholine. The excellent solution properties of the KcsA/foscholine sample at pHs ranging from 3.9 to 7.2 permitted us to discern approximately 85% of the NMR peaks in the 2D NMR spectra, using our knowledge of the 3D spectra (**Supplementary Fig. 3**). The average peak width in the proton dimension is ~25 Hz. We multiplied the data by an exponential function, a sine bell and a 75°-shifted sine bell function before Fourier transformation, and processed the results using PROSA[35]. All three datasets were used in the analysis. The spectrum with an exponential window function was used to obtain the greatest sensitivity (it was up to two-fold more sensitive) and the spectrum with the shifted sine bell function was used for the highest resolution. The sequential assignment was obtained from a combination of NOESY, HNCA and TROSY spectra of amino acid–specifically labeled samples using CARA (http://www.nmr.ch). Linewidth analysis was also done with CARA. The ^{3}J(HN,Hα) scalar couplings of tyrosine residues were measured with ^{15}N-Tyr KcsA(tox) using a quantitative constant-time ZQ-TROSY experiment described in **Supplementary Figure 6** and **Supplementary Methods** online.

Note: Supplementary information is available on the Nature Structural & Molecular Biology website.

ACKNOWLEDGMENTS

This work was supported in part by the US National Institutes of Health (GM74929 and GM56653). R.R. is a Pew Scholar and the Helen McLoraine Development Chair in Neurobiology. K.A.B. would like to thank the American Heart Association for fellowship support.

AUTHOR CONTRIBUTIONS

K.A.B. and C.T. prepared KcsA; K.A.B., C.T., W.K. and R.R. collected and analyzed NMR data; K.A.B., C.T., S.C. and R.R. contributed to scientific discussions and prepared the manuscript.

Published online at http://www.nature.com/nsmb/
Reprints and permissions information is available online at http://npg.nature.com/reprintsandpermissions

1. Hille, B. *Ion Channels of Excitable Membranes* 3rd edn. (Sinauder, Sunderland, Massachusetts, USA, 2001).
2. Doyle, D.A. *et al.* The structure of the potassium channel: molecular basis of K^+ conduction and selectivity. *Science* **280**, 69–77 (1998).
3. Jiang, Y. *et al.* Crystal structure and mechanism of a calcium-gated potassium channel. *Nature* **417**, 515–522 (2002).
4. Kuo, A. *et al.* Crystal structure of the potassium channel KirBac1.1 in the closed state. *Science* **300**, 1922–1926 (2003).
5. Jiang, Y. *et al.* X-ray structure of a voltage-dependent K^+ channel. *Nature* **423**, 33–41 (2003).
6. Shi, N., Ye, S., Alam, A., Chen, L. & Jiang, Y. Atomic structure of a Na^+ and K^+-conducting channel. *Nature* **440**, 570–574 (2006).
7. Valiyaveetil, F.I., Sekedat, M., MacKinnon, R. & Muir, T.W. Glycine as a d-amino acid surrogate in the K^+-selectivity filter. *Proc. Natl. Acad. Sci. USA* **101**, 17045–17049 (2004).
8. Bezanilla, F. & Armstrong, C.M. Negative conductance caused by entry of sodium and cesium ions into the potassium channels of squid axons. *J. Gen. Physiol.* **60**, 588–608 (1972).
9. Noskov, S.Y. & Roux, B. Importance of hydration and dynamics on the selectivity of the KcsA and NaK channels. *J. Gen. Physiol.* **129**, 135–143 (2007).
10. Perozo, E., Cortes, D.M. & Cuello, L.G. Structural rearrangements underlying K^+-channel activation gating. *Science* **285**, 73–78 (1999).
11. Heginbotham, L., LeMasurier, M., Kolmakova-Partensky, L. & Miller, C. Single *Streptomyces lividans* K^+ channels: functional asymmetries and sidedness of proton activation. *J. Gen. Physiol.* **114**, 551–560 (1999).
12. Liu, Y.S., Sompornpisut, P. & Perozo, E. Structure of the KcsA channel intracellular gate in the open state. *Nat. Struct. Biol.* **8**, 883–887 (2001).
13. Jiang, Y. *et al.* The open pore conformation of potassium channels. *Nature* **417**, 523–526 (2002).
14. Cordero-Morales, J.F. *et al.* Molecular determinants of gating at the potassium-channel selectivity filter. *Nat. Struct. Mol. Biol.* **13**, 311–318 (2006).

15. Valiyaveetil, F.I., Sekedat, M., MacKinnon, R. & Muir, T.W. Structural and functional consequences of an amide-to-ester substitution in the selectivity filter of a potassium channel. *J. Am. Chem. Soc.* **128**, 11591–11599 (2006).
16. Proks, P., Capener, C.E., Jones, P. & Ashcroft, F. Mutations within the P-loop of Kir6.2 modulates the intraburst kinetics of the ATP-sensitive potassium channel. *J. Gen. Physiol.* **118**, 341–353 (2001).
17. Berneche, S. & Roux, B. Energetics of ion conduction through the K^+ channel. *Nature* **414**, 73–77 (2001).
18. MacKinnon, R., Cohen, S.L., Kuo, A., Lee, A. & Chait, B.T. Structural conversion in prokaryotic and eukaryotic potassium channels. *Science* **280**, 106–109 (1998).
19. Chill, J.H., Louis, J.M., Miller, C. & Bax, A. NMR study of the tetrameric KcsA potassium channel in detergent micelles. *Protein Sci.* **15**, 684–698 (2006).
20. Pervushin, K., Riek, R., Wider, G. & Wuthrich, K. Attenuated T2 relaxation by mutual cancellation of dipole-dipole coupling and chemical shift anisotropy indicates an avenue to NMR structures of very large biological macromolecules in solution. *Proc. Natl. Acad. Sci. USA* **94**, 12366–12371 (1997).
21. Zhou, Y., Morais-Cabral, J.H., Kaufman, A. & MacKinnon, R. Chemistry of ion coordination and hydration revealed by the K^+ channel-Fab complex at 2.0 Å resolution. *Nature* **414**, 43–48 (2001).
22. Cortes, D.M., Cuello, L.G. & Perozo, E. Molecular architecture of full-length KcsA: role of cytoplasmic domains in ion permeation and activation gating. *J. Gen. Physiol.* **117**, 165–180 (2001).
23. Cuello, L.G., Romero, J.G., Cortes, D.M. & Perozo, E. pH-dependent gating in the Streptomyces lividans K^+ channel. *Biochemistry* **37**, 3229–3236 (1998).
24. Lu, T. *et al.* Probing ion permeation and gating in a K^+ channel with backbone mutations in the selectivity filter. *Nat. Neurosci.* **4**, 239–246 (2001).
25. Wuthrich, K. *NMR of Proteins and Nucleic Acids* (Wiley, Indianapolis, 1986).
26. Takeuchi, K., Takahashi, H., Kawano, S. & Shimada, I. Identification and characterization of the slowly exchanging pH-dependent conformational rearrangement in KcsA. *J. Biol. Chem.* **282**, 15179–15186 (2007).
27. Noskov, S.Y. & Roux, B. Ion selectivity in potassium channels. *Biophys. Chem.* **124**, 279–291 (2006).
28. Luzhkov, V.B. & Aqvist, J. A computational study of ion binding and protonation states in the KcsA potassium channel. *Biochim. Biophys. Acta* **1481**, 360–370 (2000).
29. Bucher, D., Guidoni, L. & Roethlisberger, U. The protonation state of the Glu-71/Asp-80 residues in the KcsA potassium channel. A first-principles QM/MM molecular dynamics study. *Biophys. J.* **93**, 2315–2324 (2007).
30. Zhou, Y. & MacKinnon, R. The occupancy of ions in the K^+ selectivity filter: charge balance and coupling of ion binding to a protein conformational change underlie high conduction rates. *J. Mol. Biol.* **333**, 965–975 (2003).
31. VanDongen, A.M. K channel gating by an affinity-switching selectivity filter. *Proc. Natl. Acad. Sci. USA* **101**, 3248–3252 (2004).
32. LeMaster, D.M. & Richards, F.M. NMR sequential assignment of *Escherichia coli* thioredoxin utilizing random fractional deuteriation. *Biochemistry* **27**, 142–150 (1988).
33. Marley, J., Lu, M. & Bracken, C. A method for efficient isotopic labeling of recombinant proteins. *J. Biomol. NMR* **20**, 71–75 (2001).
34. Salzmann, M., Wider, G., Pervushin, K. & Wuthrich, K. Improved sensitivity and coherence selection for [^{15}N,^{1}H]-TROSY elements in triple resonance experiments. *J. Biomol. NMR* **15**, 181–184 (1999).
35. Guntert, P., Dotsch, V., Wider, G. & Wuthrich, K. Processing of multi-dimensional NMR data with the new software PROSA. *J. Biomol. NMR* **2**, 619–629 (1992).